



Universiteit  
Leiden  
The Netherlands

## **spFRET studies of nucleosome dynamics modulated by histone modifications, histone variants and neighboring nucleosomes**

Buning, R.

### **Citation**

Buning, R. (2015, January 15). *spFRET studies of nucleosome dynamics modulated by histone modifications, histone variants and neighboring nucleosomes*. *Casimir PhD Series*. Retrieved from <https://hdl.handle.net/1887/31477>

Version: Not Applicable (or Unknown)

License: [Leiden University Non-exclusive license](#)

Downloaded from: <https://hdl.handle.net/1887/31477>

**Note:** To cite this publication please use the final published version (if applicable).

Cover Page



Universiteit Leiden



The handle <http://hdl.handle.net/1887/31477> holds various files of this Leiden University dissertation.

**Author:** Buning, Ruth

**Title:** spFRET studies of nucleosome dynamics modulated by histone modifications, histone variants and neighboring nucleosomes

**Issue Date:** 2015-01-15

## CHAPTER 2

# **Making spFRET experiments with nucleosomes succeed**

Ruth Buning and John van Noort

## 2.1 Introduction

Probing nucleosomes with spFRET (single-pair Fluorescence, or Förster, Resonance Energy Transfer) can be very informative and seems straightforward. The Förster radius is generally in the order of 5 nm, ideal for measuring the dynamics of nucleosomes that have a diameter of  $\sim 10$  nm. Nucleosomal DNA (or histones) can be labeled with a FRET-pair, reconstituted into nucleosomes and subsequently diluted to pmol concentrations to measure donor and acceptor intensities in single nucleosomes with confocal microscopy. The resulting FRET efficiency distributions should then reveal variations in nucleosome conformation.

In practice, the experiments and the interpretation of their results are far from trivial. Nucleosome instability during storage and sample preparation, sample heterogeneity, and simplifications in the analysis of fluorescence data can introduce artifacts or obscure the underlying conformational behavior of nucleosomes. All studies on single nucleosomes that aimed to discover nucleosome conformational dynamics in varying conditions and environments have encountered similar challenges regarding dilution, buffer conditions and surface interactions, for example as published in [37, 41, 55, 56].

Under optimal conditions nucleosomes remain stable, i.e. they do not dissociate, show the same behavior over the duration of the experiment, and measurements are reproducible. Experiments are preferably done in conditions where nucleosome behavior can be detected that has some biological relevance. Sample preparation of nucleosomes for single-molecule experiments is however not straightforward. Copying the protocols from one experiment to another is not always possible, for example when using nucleosomes with a different histone composition. Nevertheless, we saw that nucleosomes under optimal conditions can be stable for years (figure 2.1), depending on the specific histone composition, nucleosome concentration, and buffer conditions. In this chapter, we describe the caveats that we encountered during the single-molecule experiments described in this thesis, and present solutions or suggestions how to deal with them.

## 2.2 Reconstitution of nucleosomes with FRET pairs

### 2.2.1 DNA substrate

All DNA substrates described in this thesis are obtained by PCR (Polymerase Chain Reaction) and contain the 601 nucleosome positioning sequence [33]<sup>1</sup> (see figure 2.2).

---

<sup>1</sup>CTGGAGAATCCCGGTGCCGAGGCCGCTCAATTGGTCGTAGACAGCTCTAGCACCGCTTAAACGCACGT-ACGCGCTGTCCCCCGCGTTTTAACCGCCAAGGGGATTACTCCCTAGTCTCCAGGCACGTGTCAGATATATACATCCTGT

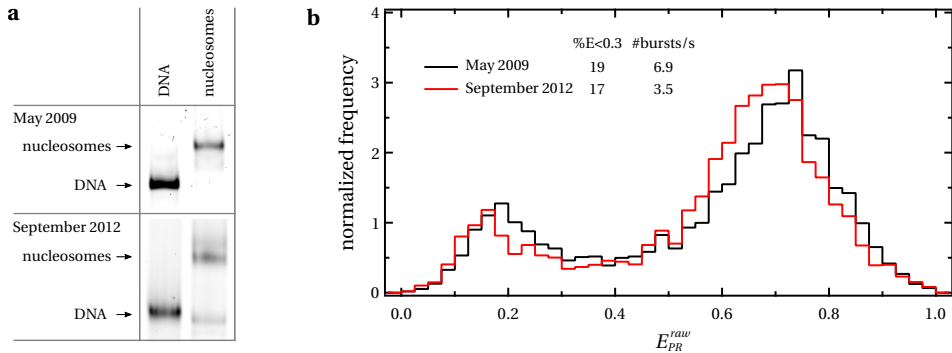


**Figure 2.1** – The same nucleosome reconstitution measured twice, with an interval of more than three years. **a**: Acceptor fluorescence image of a 5 % polyacrylamide gel with DNA and reconstituted nucleosomes. After three years, a small fraction of free DNA can be observed. **b**: FRET efficiency distribution inside the nucleosome bands shown in **a**. Population sizes with and without FRET have not changed (error margin 4 %). Shifts in FRET efficiency values are due to re-alignment of the setup. Nucleosomes were reconstituted with chicken erythrocyte histone octamers.

Fluorescent labels are easily incorporated by using fluorescently labeled primers in the PCR reaction.

Label positions that allow for the detection of nucleosomal DNA unwrapping from the nucleosome ends require the use of long, i.e. about 80 bp, primers. A detailed protocol for choosing label positions and the PCR reaction can be found in [34]. PCR reactions with primers this long are likely to produce suboptimal yields and/or by-products. The PCR products were therefore always analyzed with gel electrophoresis. If, despite optimizing the PCR conditions and standard PCR purification procedures, unwanted by-products remain, the desired product can be extracted from the gel after electrophoresis. However, UV illumination, used for imaging of DNA to facilitate the excision of gel bands, can cause nicks in the DNA. DNA substrates containing only one of the fluorescent labels, for example the free primers or substrates where one of the fluorophores is bleached, may strongly bias ensemble measurements, though do not interfere with spFRET experiments that use Alternating Laser Excitation (ALEX). It is therefore not necessary to remove these side products for spFRET experiments. Nevertheless, the long primers and the resulting nonuniform mixture of PCR products require special attention during PCR and gel analysis.

If the desired DNA construct is significantly longer than the 147 bp that forms the nucleosome core, a single PCR is not sufficient to incorporate both labels within the nucleosome. We obtained DNA fragments containing more than ~50 bp linker DNA in addition to the fluorescently labeled nucleosome positioning sequence by ligation of multiple PCR products. To minimize losses due to the formation of alternative ligation

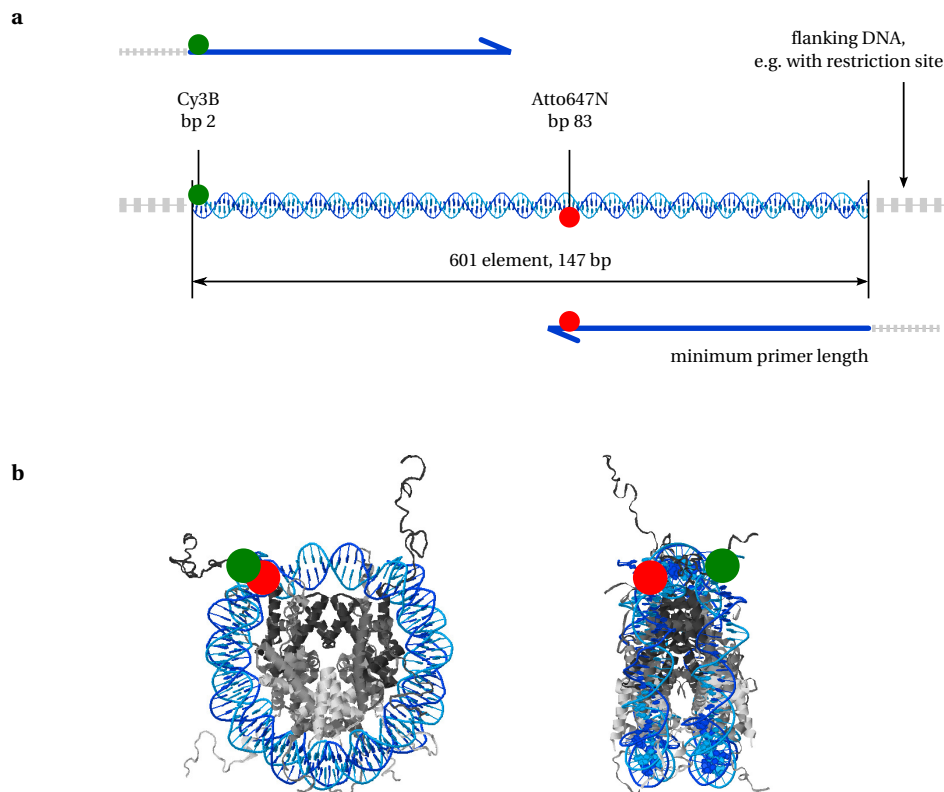


**Figure 2.2 – a:** DNA construct for mononucleosomes. All constructs described in this thesis are based on the 601 positioning sequence. The 147 bp of nucleosomal DNA are shown, with flanking DNA in grey dashes. The flanking DNA can contain restriction sites to allow subsequent digestion and ligation, or biotin or antidigoxigenin for immobilization. Fluorescent labels are incorporated in the nucleosomal DNA by PCR with fluorescently labeled primers. The fluorescent labels are ~24 nm apart in the DNA substrate, yielding no FRET. In reconstituted nucleosomes, the labels are only several nm apart, resulting in FRET efficiencies above 0.5. Label positions can be chosen at other locations in the nucleosome, different than shown here, to reveal DNA breathing more internally to the nucleosome. Unless mentioned otherwise, the nucleosome constructs presented in this chapter are fluorescently labeled at the positions indicated here. **b:** Top and side view of the crystal structure of the nucleosome core particle (1KX5, [12]), consisting of 147 bp DNA wrapped around the histone octamer, including FRET labels.

products, we used non-palindromic restriction sites.

spFRET on nucleosomes puts high demands on the homogeneity of the samples, as one wants to unequivocally attribute differences in FRET to conformational changes rather than different sample compositions. The more complicated DNA constructs required more digestion and ligation steps. Every digestion, ligation and purification step has a limited yield and causes loss of material. Five steps with 90 % yield already result in a loss of 40 % of the initial material. Therefore, a compromise was found between the purity of the sample and the amount of material.

Other methods to obtain DNA substrates include: annealing of multiple oligomers [57], restriction of the desired fragment from plasmids, or purification from native DNA, though the latter two methods lack the possibility to make use of modified oligomers to incorporate fluorophores. Alternative to fluorescently labeling the DNA molecule with a donor and an acceptor fluorophore, one or two of the labels could be placed on the histones [35, 36, 58, 59]. However, since all histones are present in duplo in each nucleosome, this method yields also complex mixtures.

Thus, though well established and straightforward techniques can be used to prepare DNA substrates for spFRET nucleosomes, the large number of preparation steps and the incomplete yields of each step make it far from straightforward to prepare enough homogeneous DNA material for reconstitution of FRET-labeled nucleosomes.

## 2.2.2 Nucleosome reconstitution

Nucleosomes can be reconstituted from DNA and histone octamers by salt gradient dialysis as described in [34]. DNA and histone octamers (HO) were mixed in various molar ratios to optimize the reconstitution yield. A high quality reconstitution product contains negligible amounts of bare DNA, which manifests itself as a single sharp band of reconstituted nucleosomes after native polyacrylamide gel electrophoresis (PAGE). The optimal molar ratio [DNA substrate]:[HO] is determined empirically and lies typically between 1:1 and 1:2 for mononucleosomes. Too high [HO] results in the formation of aggregates and acceptor quenching, shown in bulk fluorescence spectra (see figure 2.8).

Not only the molar ratio [DNA substrate]:[HO], also the total amount of DNA in the reconstitution reaction determines the quality of the reconstitution product. In general, the higher the total DNA concentration, the higher the reconstitution quality. For better reconstitution yields, competitor DNA is often added to the reconstitution reaction. Competitor DNA acts as a 'buffer' to capture superfluous HO to prevent the formation of aggregates. High DNA concentrations also help to minimize negative effects imposed by low concentrations and surface interactions (see sections 2.4.1 and 2.4.3). In our experience, a minimum of 100 nM of DNA substrate and a total amount of DNA (substrate plus competitor DNA) of 1-4  $\mu\text{g}$  in 40  $\mu\text{l}$  is optimal.

Before spFRET, we analyzed the reconstitution quality with ensemble methods. We determined the average FRET efficiency of the sample with bulk fluorescence spectroscopy. We used polyacrylamide gel electrophoresis (PAGE) to determine the relative concentrations of bare DNA and nucleosomes. All fluorescently labeled species, as well as their FRET efficiencies, can be visualized when the polyacrylamide gel is imaged with a fluorescence imager. While PAGE analysis clearly resolves subpopulations in the sample, it can affect nucleosome integrity, as discussed in section 2.3. Bulk fluorescence measured in a cuvette minimally disturbs the sample and proved to be an easy and quick reconstitution check. The combination of the two techniques yields a full, though ensemble averaged, characterization of the reconstitution.

When the DNA ligation contains side-products, and/or the reconstitution quality is too low, one could purify fully reconstituted nucleosomes from incomplete nucleosomes and bare DNA by ion exchange chromatography [60], gel electrophoresis or sucrose gradient purification [33, 61]. However, since 50-99% of material can be lost in such purification processes, even larger amounts of start material are required. Alternatively, single-molecule experiments can be performed directly inside the gel, without extraction of nucleosomes, using the gel to separate nucleosomes from other species [42, 62].

## 2.3 Nucleosomes in a polyacrylamide gel

Nucleosome reconstitutions were analyzed with 5% native polyacrylamide gel electrophoresis (PAGE). A sample of 2-8  $\mu$ l of reconstitution product was loaded on the gel (typically 29:1 bis:acrylamide, 0.2  $\times$  TB, Amersham Bioscience Hoefer SE 400 vertical gel slab unit). The gel was run at 19 V/cm at 7  $^{\circ}$ C for 90-120 minutes to separate nucleosomes from free DNA. We used fluorescence imaging for fast and accurate determination of the relative amounts of material in the bands as well as their FRET efficiencies (see section 2.6). Subsequently, we did spFRET experiments in the same gel. In some cases we observed disruptive effects of the polyacrylamide gel on the nucleosomes (see figure 2.3). Nucleosome concentrations in the gel typically drop below a nM, as measured by the burst rate, which would lead to dilution-driven dissociation. At this point it is not clear what determines the delicate balance between dilution driven dissociation, gel matrix induced disruption, and the effect of the gel matrix acting as a crowding agent, which would help to prevent dilution-driven dissociation to some extent.

Disruption inside the gel appeared to be very much dependent on the histone content. Nucleosomes reconstituted with chicken erythrocyte histone octamers (HO) and recombinant *Xenopus* Leavis HO showed slightly enhanced dissociation in the gel in some cases. Nucleosomes reconstituted with recombinant *Arabidopsis thaliana* HO showed severe dissociation in the gel. However, *Arabidopsis thaliana* nucleosomes



containing H2A.Z instead of H2A were more stable, as shown in figure 2.3b. Thus, in-gel spFRET experiments cannot be interpreted unambiguously.

## 2.4 Sample preparation for spFRET

### 2.4.1 Dilution to single-molecule concentrations

To measure single nucleosomes in a confocal microscope, the concentration of (fluorescently labeled) nucleosomes should be in the order of pM. Such sub-nM concentrations of nucleosomes and low ionic strengths however, seem to be quite remote from the conditions found *in vivo*. Moreover, dilution to sub-nM concentrations promotes dissociation of the nucleosomes [56,63]. Addition of crowding agents to the buffer and low ionic strengths prevent this dissociation. A straightforward solution to measure spFRET is to use a high concentration of nucleosomes (10-100 nM), where only a fraction of the nucleosomes is fluorescently labeled. A study that uses this principle to combine bulk and single-molecule measurements under exactly the same conditions is described in detail in [63]. In the experiments described in this thesis, we follow this strategy and keep the nucleosome concentration relatively high by adding unlabeled nucleosomes to the sample. The unlabeled nucleosomes should have the same histone composition as the labeled nucleosomes in such experiments, because histone proteins, especially the H2A-H2B dimers, can exchange between nucleosomes.

Single-molecule experiments inside a polyacrylamide gel have similar constraints. The nucleosome concentration in the band should be low enough to detect individual nucleosomes. Unlabeled nucleosomes can also be added to the gel, but they should run together with the labeled nucleosomes and should therefore have the same DNA length and position of the nucleosome. Single-molecule experiments in solution do not require identical DNA in the labeled and unlabeled nucleosomes and can therefore more easily be diluted. In both methods it is important to be aware of undesired nucleosome dissociation.

The labeled nucleosome concentration after reconstitution can be determined by the bulk fluorescence signal of the acceptor (neglecting dissociation and incomplete reconstitution). This is not necessarily the same as the DNA input concentration. In general, the nucleosome concentration is much lower after reconstitution as nucleosomes are lost during the reconstitution reaction due to sticking to surfaces. The labeled nucleosome concentration in the spFRET sample can be estimated from the burst rate. Typically, five bursts per second, with an average burst duration of 2 ms and a detection volume of a femtoliter, corresponds to ~20 pM. Thus, labeled nucleosomes can and need to be diluted with unlabeled nucleosomes to pM concentrations for spFRET.

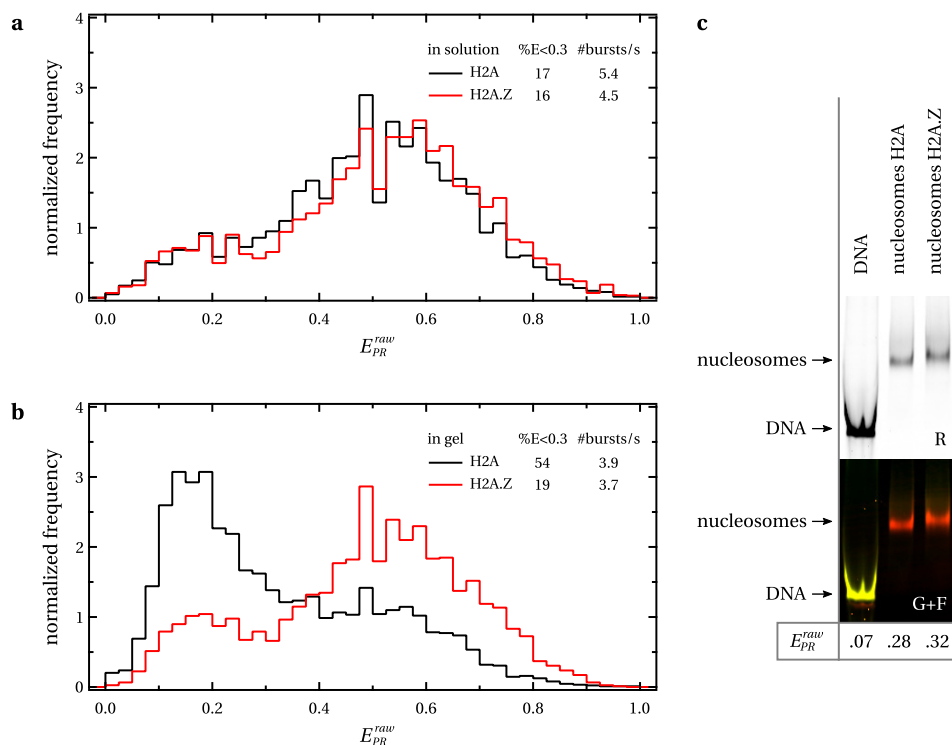


**Figure 2.3** – FRET efficiency distributions of mononucleosomes reconstituted with canonical H2A or the variant H2A.Z of *Arabidopsis Thaliana* histones. **a**: single-molecule experiments in solution; **b**: single-molecule experiments in 5% PA gel shown in **c**. Where we expect a smaller population without FRET in the gel due to separation from free DNA, the population without FRET is highest in the gel which we attribute to disruption of the nucleosomes after electrophoresis. Nucleosomes containing H2A are more susceptible to disruption in the gel than nucleosomes containing H2A.Z. The data shown here is for nucleosomes with FRET labels 27 bp from the nucleosome exit.

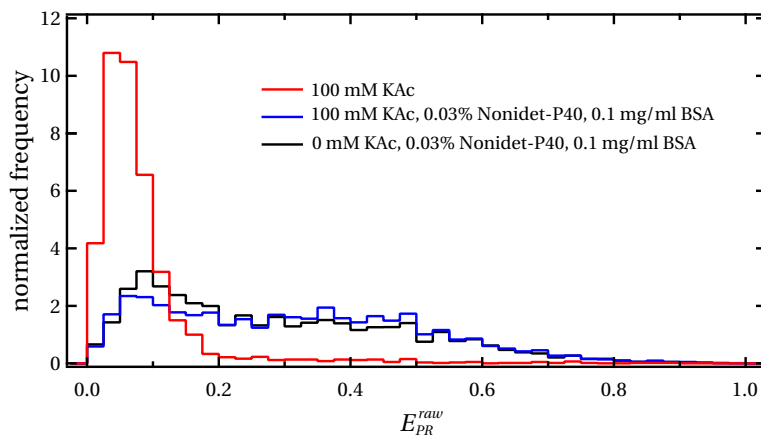


**Figure 2.4** – FRET efficiency distribution of mononucleosomes in solution at zero and at 100 mM monovalent salt. Addition of BSA and Nonidet P-40 prevents dissociation at 100 mM salt. Nucleosome concentration is around 10 pM.

## 2.4.2 Buffer conditions

Buffer conditions have a large effect on both the nucleosome integrity, and the optical performance of the fluorescent dyes. Typically, nucleosomes are kept in 10 mM Tris.HCl pH 8. Depending on the desired measurement conditions, mono- or divalent salts can be added. For example, nucleosome-nucleosome interactions require the presence of several mM magnesium ions (see chapter 5 of this thesis). However, at sub-nM nucleosome concentrations, 100 mM of monovalent salt, approaching *in vivo* conditions, can be enough to lose all FRET, indicating dissociation of the nucleosomes.

This problem is relieved by adding Nonidet P-40 and BSA, as shown in figure 2.4. BSA acts as a crowding agent to prevent dilution-driven dissociation. The anionic detergent Nonidet P-40 (also known as IGEPAL CA-630) has been found to increase the reproducibility of experiments with nucleosomes, indicating a stabilizing effect, and to prevent nucleosome precipitation [42, 55]. In this thesis, we used 0 or 50 mM NaCl, as a compromise between stability and physiological relevance.

To prevent photobleaching and -blinking of the fluorophores, an oxygen scavenger system was added to the nucleosome sample. We initially used catalase, glucose oxidase and glucose, combined with trolox. We found however that the addition of trolox only was sufficient to yield negligible amounts of photobleaching and -blinking events. Therefore, the catalase, glucose oxidase and glucose was usually omitted.

Buffer conditions inside a polyacrylamide gel are restricted by the physical properties of the gel. Proteins like BSA, catalase and glucose oxidase can not freely enter the gel matrix. Nonidet P-40 is also not compatible with in-gel experiments. Salts and

trolox can on the other hand be used without problems. However, the addition of moderate salt concentrations (10-500 mM) in absence of BSA and Nonidet P-40 leads to nucleosome dissociation, which could only be prevented by high levels of unlabeled nucleosomes (~100 nM) in the corresponding gel band.

Overall, the stability constraints of nucleosomes require careful optimization of the buffer conditions, which can be different for different nucleosome types and measurement methods.

### 2.4.3 Surface effects

During sample preparation and experiments, nucleosomes are exposed to surfaces like eppendorf tubes, pipet-tips, dialysis tubes for reconstitutions and microscope slides. Such surface exposure has a detrimental effect, as nucleosomes stick and/or dissociate near a surface [41]. The resulting drop in nucleosome concentration can be as large as tens of percents, and can in turn result in additional, dilution-driven, dissociation. The lower the initial nucleosome concentration, the larger the relative effect of the surfaces. Especially when working with concentrations below 10 nM and with relatively large surface areas (pipetting, ~ $\mu$ l sample volumes), it was essential to minimize surface interactions by using non-stick or silanized tubes and pipet-tips. Vortexing and shaking of nucleosome samples during transport further increased surface exposure and was avoided when possible. An example of (dilution driven) dissociation caused by increased surface exposure is shown in figure 2.5.

spFRET with nucleosomes in solution was measured 25  $\mu$ m above the microscope slide surface. This height however was not always sufficient to prevent surface induced dissociation of nucleosomes. Surface passivation by coating with starPEG was effective to prevent surface driven dissociation, as shown in figure 2.6. Interestingly, we found that the susceptibility of nucleosomes to surface interactions depends on the HO origin. It was therefore important to always evaluate the effects of surfaces on nucleosome stability.

## 2.5 Single-molecule fluorescence spectroscopy

### 2.5.1 Confocal setup

Single molecules were imaged with a home-built confocal microscope equipped with a 60  $\times$  water-immersion objective (NA=1.2, Olympus), as schematically depicted in figure 2.7a (see also [42]). A 515 nm diode pumped solid state laser (Cobolt) and a 636 nm diode laser (Power Technology) were used as excitation sources. The lasers were alternated at 20 kHz by analog modulation, either directly (636 nm), or with an AOM (515 nm; Isomet). The beams were spatially filtered with a single-mode fiber, and

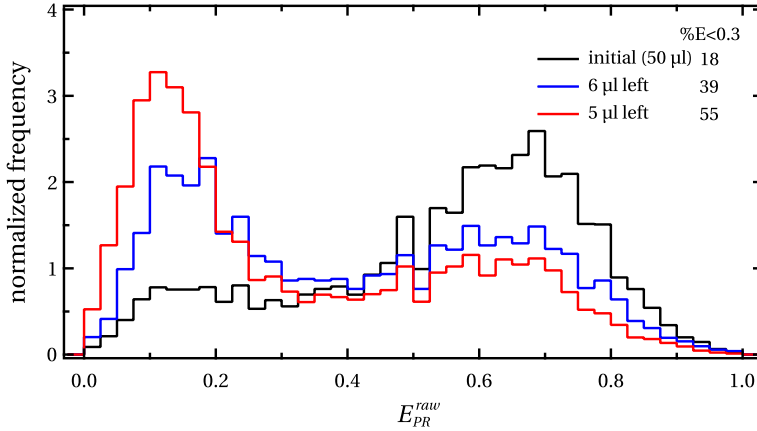


**Figure 2.5** – FRET efficiency distribution of mononucleosomes stored in normal eppendorf tubes after reconstitution. The initial volume was about 50  $\mu\text{l}$ . The population of nucleosomes without FRET increased dramatically when the total volume was reduced to a few  $\mu\text{l}$ . The lower volume in the tube results in relatively more surface-exposure, enhancing surface-induced dissociation. All measurements in 10 mM Tris.HCl pH 8.0, 0.1 mg/ml BSA, 0.03 % Nonidet P-40 and 2 mM trolox (no salt).

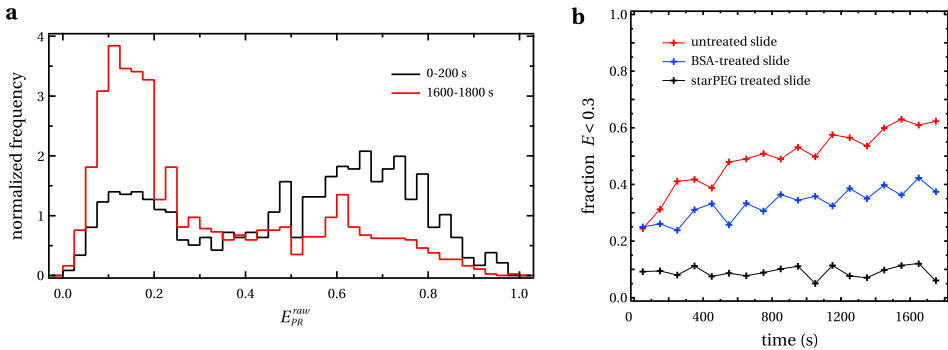


**Figure 2.6** – Increase of population of nucleosomes without FRET due to interactions with the surface of the microscope slide during a 30 minute single-molecule measurement of mononucleosomes. **a:** FRET efficiency histogram of the first and last 200 seconds of measurement on an untreated microscope slide. **b:** fraction of bursts with a proximity ratio below 0.3, as a function of time after the start of the measurement. The fraction without FRET increases on an untreated slide. Slides incubated with BSA partly prevent dissociation. On starPEG coated slides [64, 65], the fraction without FRET is stable over the measurement time (and longer, data not shown). All measurements in 10 mM Tris.HCl pH 8.0, 0.1 mg/ml BSA, 0.03 % Nonidet P-40, 2 mM trolox, 50 mM NaCl, and a 5-10-fold excess of unlabeled nucleosomes.

focussed 25  $\mu\text{m}$  above the glass-buffer interface by the objective. The excitation powers were in the order of 10  $\mu\text{W}$ . The collected fluorescence was spatially filtered with a 50  $\mu\text{m}$  pinhole in the image plane, and was split into a donor and an acceptor channel by a dichroic mirror (640dcxr, Chroma). The fluorescence was filtered with emission filters (hq570/100m for the donor channel, hq700/75m for the acceptor channel, Chroma) to minimize crosstalk, and was imaged on the active area of single photon avalanche photodiodes (SPCM AQR-14, Perkin-Elmer). The photodiodes were read out with a TimeHarp 200 photon counting board (Picoquant GmbH). Figure 2.7b shows an example of a fluorescence time trace with bursts of individual nucleosomes. In a typical experiment, data was collected for 30 minutes in which 2000-10000 bursts of fluorescence were detected.

## 2.5.2 Single-molecule burst selection

A burst selection algorithm is needed to distinguish fluorescence events from background. Bursts of fluorescence were detected using the method described in [66]. A burst was assigned if a minimum of 50 photons arrived subsequently, with a maximum interphoton time of 100  $\mu\text{s}$ . If the maximum interphoton time is taken too small, single bursts can be split, resulting in double counts and bursts with relatively low numbers of photons, leading to broadening of the FRET efficiency histograms. Lowering the minimum number of photons per burst increases the number of bursts detected, but may lead to the detection of false positives and again broadening of the FRET histograms. If it is taken too high, bursts will be missed.

## 2.5.3 Caveats in spFRET

Though the principle of burst detection and classification seems to be straightforward, it can be prone to multiple complications. Burst selection criteria were chosen to minimize false negatives, i.e. missed bursts, and false positives, i.e. fluctuations in background intensity mistakenly marked as bursts, which would both lead to broadening and shifting of FRET distributions.

Another artifact arises when individual particles pass the detection volume multiple times. This will be detected as multiple bursts and leads to double (or more) counts of the same particle, which is undesired. It can however be turned to an advantage and used as a tool to detect dynamics at timescales longer than the diffusion time ( $\sim 2$  ms in solution,  $\sim 4$  ms in gel), with so-called recurrence analysis of single particles (RASP), developed by Hoffmann et al [67]. Here we ignored possible multi-passage bursts.

Making use of Alternating Laser EXcitation (ALEX), we determined not only the FRET efficiency, but also the label stoichiometry for every burst [43]. This allows sorting into doubly labeled (Donor (D) + Acceptor (A)) and Donor-only and Acceptor-only

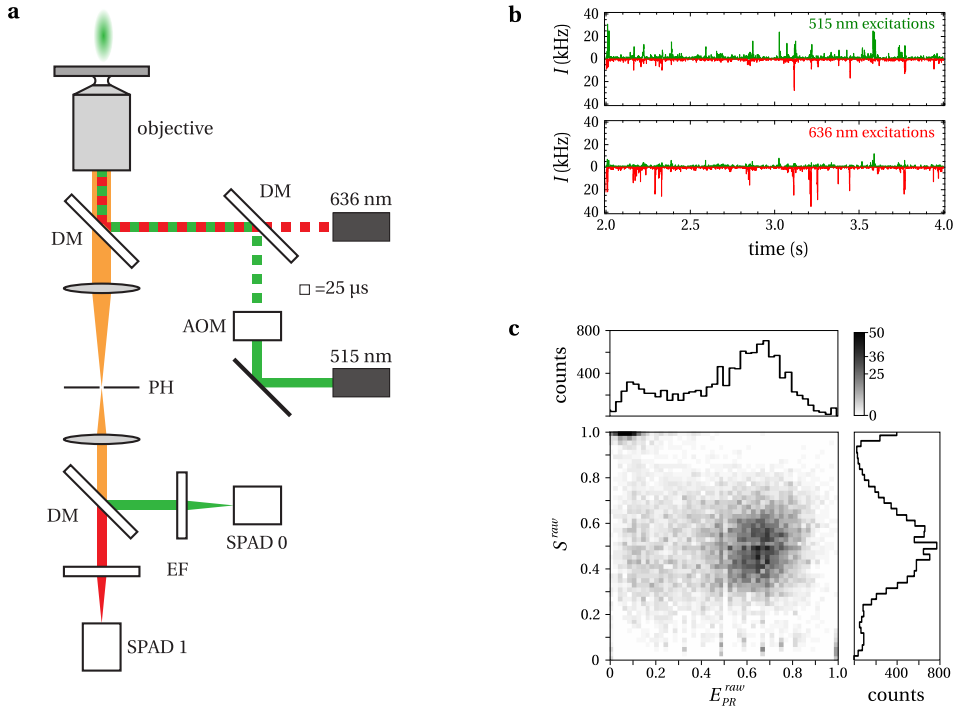


**Figure 2.7 – a:** Schematic overview of the confocal FRET microscope. DM: dichroic mirror; AOM: acousto-optical modulator; PH: pinhole; EF: emission filter; SPAD: single photon avalanche diode. The lasers are alternated at 20 kHz by analog modulation either directly (636 nm laser) or with an AOM (515 nm laser) and synchronized with the 10 MHz clock on the photon counting board. The resulting fluorescence from freely diffusing molecules in the excitation volume is collected by the objective, filtered through an emission filter, and spatially filtered through a pinhole. Donor and acceptor fluorescence are imaged on different SPADs after passing a dichroic mirror. **b:** Typical fluorescence intensity timetraces of the four different photon streams acquired with the setup in a. Photon arrival times are binned to 1 ms. Bursts of fluorescence arise from the passage of a single particle through the excitation volume. In a typical experiment, data was collected for 30 minutes in which 2000-10000 bursts of fluorescence were detected. **c:** Typical 2D-histogram of FRET efficiency ( $E_{PR}^{raw}$ ) and label stoichiometry ( $S^{raw}$ ) for mononucleosomes. Four populations are distinguishable: donor only ( $S^{raw} > 0.8$ ), acceptor only ( $S^{raw} < 0.2$ ), doubly labeled ( $0.2 < S^{raw} < 0.8$ ) with FRET ( $E_{PR}^{raw} > \sim 0.3$ ) and without FRET ( $E_{PR}^{raw} < \sim 0.3$ ).

bursts. D-only and A-only bursts can then be excluded from subsequent analysis. Artifacts due to the presence of D-only and A-only populations resulting from photo-bleaching are avoided in this manner. Although ALEX allows to select for D+A labeled particles, it can not distinguish between nucleosomes without FRET (that are partially unwrapped) and free DNA. The amount of free DNA should therefore be negligible, or accurately determined by for example gel electrophoresis (which is not straightforward, as described in section 2.3).

We determined for every burst the mean FRET efficiency and label stoichiometry from all photons in the burst. When all caveats are properly taken care of, the observed distribution can be split into separate populations with differing FRET efficiencies, reflecting different conformations of the nucleosome. This variation can be either static or dynamic. A burst analysis technique that resolves static from dynamic heterogeneity is presented by Tomov et al. [68]. Here, we did not discriminate between static and dynamic differences in FRET. Based on previous work [41] we anticipate the lifetimes of the open and closed conformation of the nucleosome to be 25 and 280 ms, which are both larger than the diffusion limited window of 2-4 ms we can measure here.

## 2.6 Quantitative comparison of multiple FRET techniques

Though different measurement techniques have different requirements for sample preparation, which may have a large effect on the measured FRET, we nevertheless aimed for a quantitative comparison of FRET efficiencies across setups.

### 2.6.1 Bulk fluorescence spectroscopy

The average FRET efficiency, as determined from the ensemble fluorescence spectrum, gives a general indication of the yield of the nucleosome reconstitution reaction. The sample does not need to be diluted and could be recovered from the cuvette after measuring. A typical bulk fluorescence spectrum of mononucleosomes with Cy3B and ATTO647N is shown in figure 2.8. Typically, we record two emission spectra: emission from 535 to 735 nm with donor excitation (515 nm) and emission from 635 to 735 nm with direct acceptor excitation (615 nm).

We determined the FRET efficiency from the enhanced fluorescence of the acceptor using the  $\text{ratio}_A$  method [28]:

$$E_{\text{ratio}A} = \frac{\epsilon_{615}^A}{\epsilon_{515}^D} \frac{F_{515}^A}{F_{615}^A} - \frac{\epsilon_{515}^A}{\epsilon_{515}^D} \quad (2.1)$$



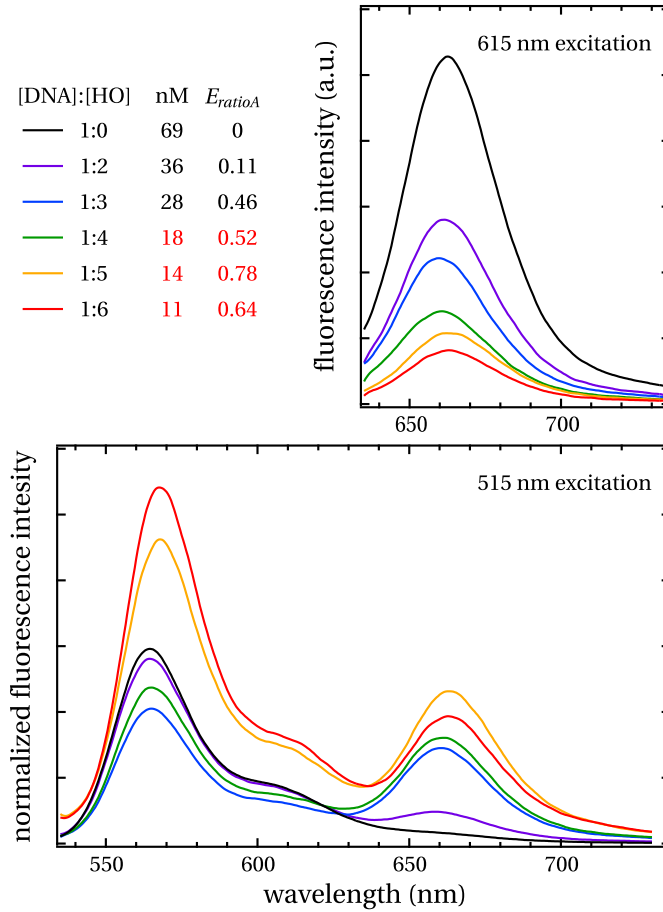


**Figure 2.8** – Bulk fluorescence spectra of mononucleosome reconstitutions. The concentration is determined from the peak fluorescence intensity with excitation at 615 nm (direct acceptor excitation). The fluorescence spectra for 515 nm excitation are normalized by dividing by the peak fluorescence intensity for 615 nm excitation. The FRET efficiency is determined from the peak intensities with excitation at 515 nm via equation 2.1. For high histone octamer (HO) concentrations, the 615 nm spectra do no longer provide an accurate concentration estimation. The nucleosome concentration is underestimated, as shown by the normalized 515 nm spectra, which lie above the lower [HO] spectra over the entire wavelength range. FRET efficiencies calculated from these spectra are not reliable, indicated by values in red. Note also the shift of the acceptor fluorescence peak to higher wavelength, like the peak for bare DNA. The optimal [DNA] to [HO] ratio depends on multiple factors, including the absolute DNA concentration and the amount of competitor DNA and can differ from what is shown here.

where  $\epsilon_{\lambda}^{A/D}$  is the donor or acceptor extinction coefficient at wavelength  $\lambda$ ,  $F_{\lambda}^A$  the fluorescence intensity of the acceptor when excited at wavelength  $\lambda$ , and  $d^+$  the fractional labeling coefficient of the donor. The fluorescence intensity of the acceptor was determined from its maximum value, which is at approximately 663 nm. To obtain the acceptor fluorescence when excited at the donor wavelength,  $F_{515}^A$ , the donor fluorescence at 663 nm, which was previously determined from the fluorescence at 663 nm of a donor-only sample and was typically found to be  $0.11 \cdot F_{515}^D$ , was subtracted.  $d^+$  was determined from DNA and fluorophore absorption peaks in an absorption spectrum of the labeled DNA.

The fluorescence intensity of the acceptor for direct acceptor excitation is a measure for the acceptor concentration, which can be calibrated with an absorption spectrum. If the amount of acceptor-only species (e.g. free primers) and free DNA in the sample is negligible, the acceptor concentration directly gives the nucleosome concentration in the sample.

At high histone octamer concentrations, the total acceptor concentration seems to drop, as shown in fluorescence spectra for direct acceptor excitation (figure 2.8). This is possibly due to the formation of aggregates accompanied by acceptor quenching. This leads to an underestimation of the nucleosome concentration and incorrect FRET efficiency calculation and normalization of 515 nm excitation spectra.

## 2.6.2 PAGE and spFRET

The definitions and descriptions how to determine FRET efficiencies and correction factors found in this section are all based on Lee et al. [31].

### 2.6.2.1 Definitions of FRET efficiencies and label stoichiometries

**Photon streams and correction factors** In any FRET experiment with excitation and detection at both the donor (D) and acceptor (A) wavelength, four experimental photon streams exist:

- D-emission upon D-excitation:  $I_{Dex}^{Dem}$
- A-emission upon D-excitation:  $I_{Dex}^{Aem}$
- D-emission upon A-excitation:  $I_{Aex}^{Dem}$
- A-emission upon A-excitation:  $I_{Aex}^{Aem}$

The A-emission upon D-excitation consists mainly of photons due to FRET ( $I^F$ ), but leakage of donor photons into the acceptor channel and direct excitation of the acceptor by the donor excitation wavelength also contribute to this signal:

$$I_{Dex}^{Aem} = I^F + l \cdot I_{Dex}^{Dem} + d \cdot I_{Aex}^{Aem} \quad (2.2)$$

The correction factors  $l$  for leakage and  $d$  for direct excitation depend on absorption cross sections, quantum efficiencies and detection efficiencies of the dyes and the detection system and can be experimentally determined from D- and A-only fractions or samples, as explained in detail in [31]:

$$l = \frac{I_{Dex}^{Aem}}{I_{Dex}^{Dem}} \quad \text{for a D-only population} \quad (2.3)$$

$$d = \frac{I_{Dex}^{Aem}}{I_{Aex}^{Aem}} \quad \text{for an A-only population} \quad (2.4)$$

Correction factor  $l$  is defined by the detection efficiencies of D-emission in the D- and A-channel, and is thus instrument-dependent. Correction factor  $d$  is determined by the photon counts of A-emission upon D- and A-excitation, and is therefore dependent on the laser intensities. Therefore,  $d$  must be determined for every measurement (series) separately, since laser intensities were varied to minimize bleaching effects and to balance the donor and acceptor signal intensities.

**FRET efficiency** The absolute FRET efficiency is given by:

$$E = \frac{I^F}{I^F + \gamma I_{Dex}^{Dem}} = \frac{I_{Dex}^{Aem} - l I_{Dex}^{Dem} - d I_{Aex}^{Aem}}{I_{Dex}^{Aem} - l I_{Dex}^{Dem} - d I_{Aex}^{Aem} + \gamma I_{Dex}^{Dem}} \quad (2.5)$$

where  $\gamma$  is a detection correction factor involving quantum yields ( $\phi$ ) and detection efficiencies ( $\eta$ ) of donor and acceptor [69, 70]:

$$\gamma = \frac{\phi_A \eta_{Aem}^A}{\phi_D \eta_{Dem}^D} \quad (2.6)$$

$\eta_{Dem}^D$  and  $\eta_{Aem}^A$  are the detection efficiencies of D-emission in the D-detection channel and A-emission in the A-detection channel.

Taking  $\gamma = 1$  gives the proximity ratio:

$$E_{PR} = \frac{I^F}{I^F + I_{Dex}^{Dem}} = \frac{I_{Dex}^{Aem} - l I_{Dex}^{Dem} - d I_{Aex}^{Aem}}{I_{Dex}^{Aem} - l I_{Dex}^{Dem} - d I_{Aex}^{Aem} + I_{Dex}^{Dem}} \quad (2.7)$$

The proximity ratio is often used instead of the absolute  $E$  to circumvent determination of  $\gamma$ . If only relative changes in the FRET efficiency histogram are of interest, the proximity ratio suffices. Differences between  $E$  and  $E_{PR}$  as a function of  $\gamma$  are most

pronounced for intermediate FRET values. To increase the resolution for low- $E$  samples, Gansen et al. [32] developed an approach that deliberately lets  $\gamma$  deviate from 1. Note that the expression for  $E_{PR}$  still involves the corrections for leakage and direct excitation. Without these correction factors, we get the most simplified expression for the FRET efficiency:

$$E_{PR}^{raw} = \frac{I_{Dex}^{Aem}}{I_{Dex}^{Aem} + I_{Dex}^{Dem}} \quad (2.8)$$

which can be directly calculated from the experimental photon streams, but depends heavily on the experimental conditions.

**Label stoichiometry** Accurate FRET measurements require dual labeling of every molecule in the sample. This can not always be achieved, especially for spFRET, in which bleaching occurs frequently. We therefore measure the label stoichiometry  $S$  in each measurement. Similar to the expressions for the FRET efficiency, Lee et al. [31] defined an  $E$ -independent stoichiometry ratio  $S_\gamma$ ; a crosstalk-corrected stoichiometry ratio  $S$ , and a raw stoichiometry ratio  $S^{raw}$ :

$$S_\gamma = \frac{I^F + \gamma I_{Dex}^{Dem}}{I^F + \gamma I_{Dex}^{Dem} + I_{Aex}^{Aem}} = \frac{I_{Dex}^{Aem} - l I_{Dex}^{Dem} - d I_{Aex}^{Aem} + \gamma I_{Dex}^{Dem}}{I_{Dex}^{Aem} - l I_{Dex}^{Dem} - d I_{Aex}^{Aem} + \gamma I_{Dex}^{Dem} + I_{Aex}^{Aem}} \quad (2.9)$$

$$S = \frac{I^F + I_{Dex}^{Dem}}{I^F + I_{Dex}^{Dem} + I_{Aex}^{Aem}} = \frac{I_{Dex}^{Aem} - l I_{Dex}^{Dem} - d I_{Aex}^{Aem} + I_{Dex}^{Dem}}{I_{Dex}^{Aem} - l I_{Dex}^{Dem} - d I_{Aex}^{Aem} + I_{Dex}^{Dem} + I_{Aex}^{Aem}} \quad (2.10)$$

$$S^{raw} = \frac{I_{Dex}^{Aem} + I_{Dex}^{Dem}}{I_{Dex}^{Aem} + I_{Dex}^{Dem} + I_{Aex}^{Aem}} \quad (2.11)$$

**Correction factor  $\gamma$**  The correction factor  $\gamma$  can be experimentally determined from the relation between  $E_{PR}$  and  $S$  for two or more populations measured under identical conditions, ideally within a single measurement. The slope ( $\Sigma$ ) and intercept ( $\Omega$ ) of the linear relation between  $E_{PR}$  and  $1/S$  define  $\gamma$ :

$$1/S = \Omega + \Sigma E_{PR} \quad (2.12)$$

$$\gamma = (\Omega - 1)/(\Omega + \Sigma - 1) \quad (2.13)$$

The correction factor  $\gamma$ , defined in equation 2.6, depends on the quantum yields, and thus on the local environment of the fluorophores (e.g. pH, temperature, incorporation site of the fluorophore), and on the detection efficiencies, which depend on

the optical alignment of the setup and the properties of optics, filters and the detectors used. Therefore, accurate comparison of experimental FRET efficiencies requires a fresh determination of  $\gamma$  for every setup, and even for every measurement series when the alignment or experimental factors have been altered.

### 2.6.2.2 Determination of correction factors

**spFRET** For the single-pair FRET experiments, determination of the correction factors is quite straightforward. The ability of ALEX to recover D-A stoichiometry enables sorting of D-only, A-only and D-A species. Population sorting allows determination of all correction factors needed in a single measurement. The sorting capability of ALEX allows accurate determination of the FRET efficiency, independent of instrumental factors (like excitation intensity and optical components/alignment). All data necessary is available from a single measurement.

$l$  follows from the D-only population: calculate  $l$  (eq. 2.3) for every burst and take the mean.

$d$  follows from the A-only population: calculate  $d$  (eq. 2.4) for every burst and take the mean.

$\gamma$  follows from two or more D+A populations with different FRET efficiency. After correcting for  $l$  and  $d$ , calculate  $E_{PR}$  (eq. 2.7) and  $S$  (eq. 2.10) for every burst and take the mean. A linear fit to  $1/S$  versus  $E_{PR}$  gives  $\gamma$  via slope and intercept (eqs. 2.12 and 2.13).

**Gel electrophoresis** For the polyacrylamide gel electrophoresis (PAGE) experiments described in 2.3, the correction factors can be estimated when a D-only and an A-only band is present in the gel.

$l$  follows from a D-only band: calculate  $l$  (eq. 2.3) from the integrated fluorescence intensities of the band (after background-subtraction).

$d$  follows from an A-only population: calculate  $d$  (eq. 2.4) from the integrated fluorescence intensities of the band (after background-subtraction).

$\gamma$  follows from two or more D+A bands with differing FRET efficiency. After correcting for  $l$  and  $d$ , calculate  $E_{PR}$  (eq. 2.7) and  $S$  (eq. 2.10) for every band. A linear fit to  $1/S$  versus  $E_{PR}$  gives  $\gamma$  via slope and intercept (eqs. 2.12 and 2.13).

A caveat when determining the correction factors for PAGE experiments is that the D-only and A-only fractions within D+A bands are unknown, which leads to an underestimation of  $\gamma$ . D-only and A-only populations can originate from bleaching of one of the fluorophores during the electrophoresis and/or imaging process.

### 2.6.2.3 Comparison of $\gamma$ across setups without absolute $\gamma$ determination

The ratio between the values of  $\gamma$  for two different setups or measurement series can be determined without knowledge of the absolute  $\gamma$  values if a FRET standard with fixed FRET efficiency is measured in both setups. It is required that the D-only population is either absent (i.e. by population sorting with ALEX-spFRET) or (assumed to be) the same for both setups/measurement series.

The absolute FRET efficiency (eq. 2.5) must be identical for both datasets (subscripts 1 and 2):

$$E = \frac{I_1^F}{I_1^F + \gamma_1 I_{Dex,1}^{Dem}} = \frac{I_2^F}{I_2^F + \gamma_2 I_{Dex,2}^{Dem}} \quad (2.14)$$

Rearrangement of eq. 2.7 gives:

$$\frac{1}{E_{PR}} - 1 = \frac{I_{Dex}^{Dem}}{I^F} \quad (2.15)$$

Rearrangement of eq. 2.14 and substitution of eq. 2.15 gives:

$$\frac{1}{E} - 1 = \gamma_1 \frac{I_{Dex,1}^{Dem}}{I_1^F} = \gamma_1 \left( \frac{1}{E_{PR,1}} - 1 \right) = \gamma_2 \left( \frac{1}{E_{PR,2}} - 1 \right) \quad (2.16)$$

from which follows:

$$\frac{\gamma_1}{\gamma_2} = \frac{E_{PR,2}(1 - E_{PR,1})}{E_{PR,1}(1 - E_{PR,2})} \quad (2.17)$$

## 2.7 Conclusions

During our spFRET investigations of nucleosomes in various conditions we encountered several difficulties. Here, we described the procedures for the preparation of nucleosome samples, the detection of spFRET with confocal fluorescence spectroscopy and the analysis of FRET efficiencies, and how we have dealt with these difficulties.

Under non-optimal conditions, complete dissociation of nucleosomes into histones and DNA, or partial dissociation into dimers and hexa- or tetramers occurs. Both are irreversible and should be avoided. Non-optimal conditions include dilution to sub-nM concentrations, high ionic strengths and surface effects, and depend on the specific histone composition and probably also the DNA sequence. Based on our experience, described in this chapter, we conclude that essential conditions for good measurements include:

- 100 % reconstitution yield (no bare DNA)
- reconstitution at high DNA concentration ( $\sim\mu\text{g}/\mu\text{l}$ ), and high volumes ( $>40\ \mu\text{l}$ ) (relatively less surface)
- measurement in solution
- addition of BSA & Nonidet P-40
- a total (labeled + unlabeled) nucleosome concentration  $> 10\ \text{nM}$
- the use of treated surfaces: non-stick tubes and passivated slides in spFRET experiments

If not only the distribution of subpopulations, but also the FRET efficiencies or label distances are desired, correction factors to the raw FRET efficiency have to be taken into account. The data and considerations presented in this chapter will help future researchers design and carry out spFRET experiments on nucleosomes and have been the basis for all experiments presented in this thesis.

